Preprints of the 19th World Congress
The International Federation of Automatic Control
Cape Town, South Africa. August 24-29, 2014

Leader-follower Pose Consensus for Heterogeneous Robot Networks with Variable Time-Delays ⋆

Carlos I. Aldana *, **Emmanuel Nuño** **, **Luis Basañez** *

* *Institute of Industrial and Control Engineering, Technical University of Catalonia. Barcelona 08028, Spain. {carlos.aldana, luis.basanez}@upc.edu.*
** *Department of Computer Science, CUCEI, University of Guadalajara. Guadalajara 44430, Mexico. emmanuel.nuno@cucei.udg.mx.*

Abstract: This paper proposes a distributed proportional plus damping (P+d) control algorithm to solve the leader-follower problem in which a network of heterogeneous robots, modeled in the operational space, has to be regulated at a given constant leader pose (position and orientation). The leader pose is only available to a certain set of followers. A singularity-free representation, unit-quaternions, is used to describe the robots orientation and the network is represented by an undirected and connected interconnection graph. Furthermore, it is shown that the controller is robust to interconnection variable time-delays. Experiments, with a network of two 6-Degrees-of-Freedom (DoF) robots, are presented to illustrate the performance of the proposed scheme.

1. INTRODUCTION

The *operational space* is a subspace of the Special Euclidean space of dimension three, denoted SE(3). It is well-known that the minimum number of coordinates required to define the *pose* of an object in a three-dimensional space is six: three for the position and three for the orientation (attitude). Operational space control becomes evident when cooperative tasks have to be described and performed by multiple robot manipulators that could be kinematically dissimilar (heterogeneous)(Liu and Chopra, 2012; Aldana et al., 2012). The practical applications of multi-robot systems span different areas such as underwater and space exploration, hazardous environments (search and rescue missions, military operations), and service robotics (material handling, furniture assembly, etc.).

The consensus problem involves the design of algorithms such that agents can reach an agreement on their states, or on a common objective. This problem has been widely studied for first and second-order *linear time invariant* systems in the generalized coordinates space, that is the case of linearized robots in the *joint space*. Some of the proposed approaches include (Hu et al., 2013) where a hybrid consensus control protocol is reported; (Sun, 2012) that deals with uncertain topologies with interconnection delays; (Abdessameud and Tayebi, 2013) that presents a partial state feedback consensus controller; and (Nuño et al., 2013) that use a proportional plus damping (P+d) control algorithm to solve the leaderless consensus problem in the joint space. For a comprehensive study and further reference along this line, the reader may refer to (Olfati-Saber and Murray, 2004). There are several interesting papers dealing with Euler-Lagrange (EL) systems in the operational space, however most of them only address the orientation part. Among these are (Liu and Chopra, 2012) where an adaptive controller is proposed to solve the leader-follower attitude-only consensus problem in networks of heterogeneous robot manipulators; (Abdessameud et al., 2012) that proposes synchronization schemes to resolve the leader-follower and leaderless problems for groups of rigid bodies in the presence of communication delays; and (Ren, 2007) where three synchronization cases for the attitude alignment of spacecrafts are presented.

Compared to the previously cited consensus solutions, this paper proposes a leader-follower consensus algorithm for networks of robots modeled in the operational space that takes into account the full pose of the robots and not only the attitude. This control scheme can be employed in non-identical heterogeneous robots with different Degrees of Freedom (DoF). The proposed controller is a simple distributed P+d algorithm that is model independent (in the sense that it is not necessary to know the robot's inertia matrix or the Coriolis forces) and is robust to interconnecting variable time-delays. Furthermore, compare to other schemes that use singular minimum orientation representations, this work employs the singularity-free unit-quaternions. Moreover, under the assumption that, at least, one follower has a direct access to the leader pose, it is shown that the proposed leader-follower controller ensures the asymptotic convergence of the robots pose to the constant leader pose and the asymptotic convergence to zero of the linear and angular velocities. Finally, an experimental validation of the leader-follower controller

⋆ This work has been partially supported by: the Mexican CONACyT doctoral grant 168998; the Mexican CONACyT project CB-129079; and the Spanish CICYT projects DPI2010-15446 and DPI2011-22471.

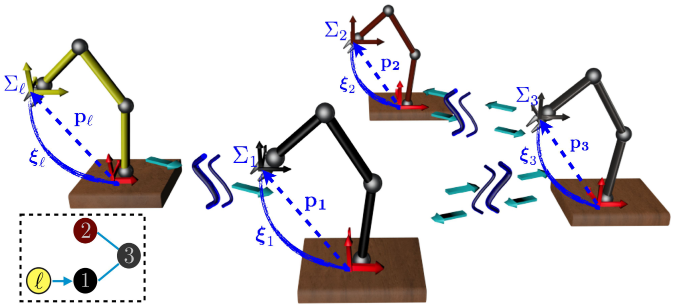

Fig. 1. Example of a robot network and the graph representing the interconnection

using a network composed of two 6-DoF robots is presented.

The following *notation* is used throughout the paper. $\mathbb{R} := (-\infty, \infty)$, $\mathbb{R}_{>0} := (0, \infty)$, $\mathbb{R}_{\geq 0} := [0, \infty)$. $|\mathbf{x}|$ stands for the standard Euclidean norm of vector $\mathbf{x}$. $\mathbf{I}_k$ and $\mathbf{\emptyset}_k$ represent, respectively, the identity and all-zeros matrices of size $k \times k$. $\mathbf{1}_k$ and $\mathbf{0}_k$ represent column vectors of size k with all entries equal to one and to zero, respectively. The spectrum of the square matrix $\mathbf{A}$ is denoted by $\sigma(\mathbf{A})$ where the minimum and the maximum of its spectrum is denoted by $\sigma_{\min}(\mathbf{A})$ and $\sigma_{\max}(\mathbf{A})$, respectively. For any matrix $\mathbf{A} \in \mathbb{R}^{n\times m}$, $\mathbf{A}^\top(\mathbf{A}\mathbf{A}^\top)^{-1}$ is its Moore-Penrose pseudo-inverse matrix denoted by $\mathbf{A}^\dagger$. For any function $\mathbf{f} : \mathbb{R}_{\geq 0} \to \mathbb{R}^n$, the $\mathcal{L}_\infty$-norm is defined as $\|\mathbf{f}\|_\infty := \underset{t\geq 0}{sup} |\mathbf{f}(t)|$, $\mathcal{L}_2$-norm as $\|\mathbf{f}\|_2 := (\int_0^\infty |\mathbf{f}(t)|^2 dt)^{1/2}$. The $\mathcal{L}_\infty$ and $\mathcal{L}_2$ spaces are defined as the sets $\{\mathbf{f} : \mathbb{R}_{\geq 0} \to \mathbb{R}^n : \|\mathbf{f}\|_\infty < \infty\}$ and $\{\mathbf{f} : \mathbb{R}_{\geq 0} \to \mathbb{R}^n : \|\mathbf{f}\|_2 < \infty\}$, respectively. The argument of all time dependent signals is omitted, *e.g.*, $\mathbf{x} \equiv \mathbf{x}(t)$, except for those which are time-delayed, *e.g.*, $\mathbf{x}(t - T(t))$. The subscript $i \in \bar{N} := \{1, ..., N\}$, where N is the number of followers nodes of the network.

2. SYSTEM MODEL

The complete dynamical description of the system contains two basic elements: i) the dynamics of the nodes and; ii) the interconnection of the nodes. It is assumed that each follower node contains a fully-actuated, revolute joints robot manipulator and that the interconnection of the network can be represented using graph theory. Fig. 1 shows an example of a robot network with a followers network compose by three robots.

2.1 Dynamics of the nodes

Every ith-node is modeled as a n_i-DoF robot manipulator, where $i \in \bar{N}$. Its EL-equation of motion, in joint space, is given by

$$\bar{\mathbf{M}}_i(\mathbf{q}_i)\ddot{\mathbf{q}}_i + \bar{\mathbf{C}}_i(\mathbf{q}_i, \dot{\mathbf{q}}_i)\dot{\mathbf{q}}_i + \bar{\mathbf{g}}_i(\mathbf{q}_i) = \boldsymbol{\tau}_i \tag{1}$$

where $\mathbf{q}_i, \dot{\mathbf{q}}_i, \ddot{\mathbf{q}}_i \in \mathbb{R}^{n_i}$, are the joint positions, velocities and accelerations, respectively; $\bar{\mathbf{M}}_i(\mathbf{q}_i) \in \mathbb{R}^{n_i\times n_i}$ is the symmetric and positive definite inertia matrix; $\bar{\mathbf{C}}_i(\mathbf{q}_i, \dot{\mathbf{q}}_i) \in \mathbb{R}^{n_i\times n_i}$ is the Coriolis and centrifugal effects matrix, defined via the Christoffel symbols of the first kind; $\bar{\mathbf{g}}_i(\mathbf{q}_i) \in \mathbb{R}^{n_i}$ is the gravitational torques vector and $\boldsymbol{\tau}_i \in \mathbb{R}^{n_i}$ is the torque exerted by the actuators (motors). Note that since the robots are heterogeneous they can have different numbers of DoF, i.e., $n_i \neq n_j$, for $j \neq i$, and $j \in \bar{N}$. The pose of the ith-end-effector, relative to a common reference frame, is denoted by the vector $\mathbf{x}_i \subset \mathbb{R}^7$ and it contains the position vector $\mathbf{p}_i \in \mathbb{R}^3$ and the orientation unit-quaternion [1] $\boldsymbol{\xi}_i \in S^3$, such that $\mathbf{x}_i := [\mathbf{p}_i^\top, \boldsymbol{\xi}_i^\top]^\top$. See Fig. 1 for the location of the reference frames and the pose vectors in an example scenario.

The relation between the joint velocities $\dot{\mathbf{q}}_i$ and the linear $\dot{\mathbf{p}}_i$ and angular $\boldsymbol{\omega}_i$ velocities of the ith-end-effector, expressed also relative to a common reference frame, is given by

$$\boldsymbol{\upsilon}_i = \begin{bmatrix} \dot{\mathbf{p}}_i \\ \boldsymbol{\omega}_i \end{bmatrix} = \mathbf{J}_i(\mathbf{q}_i)\dot{\mathbf{q}}_i \tag{2}$$

where $\boldsymbol{\upsilon}_i \in \mathbb{R}^6$ and $\mathbf{J}_i(\mathbf{q}_i) \in \mathbb{R}^{6\times n_i}$ is the *geometric Jacobian* matrix. Using the principle of the virtual work, the following relation between joint torque $\boldsymbol{\tau}_i$ and the Cartesian forces $\mathbf{f}_i$ is obtained

$$\boldsymbol{\tau}_i = \mathbf{J}_i^\top(\mathbf{q}_i)\mathbf{f}_i, \tag{3}$$

where $\mathbf{f}_i \in \mathbb{R}^6$, $\mathbf{f}_i := [\mathbf{h}_i^\top, \mathbf{m}_i^\top]^\top$ and $\mathbf{h}_i, \mathbf{m}_i \in \mathbb{R}^3$ represent the Cartesian forces and moments, respectively. Pre-multiplying (2) by the Jacobian pseudo-inverse $\mathbf{J}_i^\dagger(\mathbf{q}_i)$ and differentiating, yields

$$\ddot{\mathbf{q}}_i = \mathbf{J}_i^\dagger(\mathbf{q}_i)\dot{\boldsymbol{\upsilon}}_i + \dot{\mathbf{J}}_i^\dagger(\mathbf{q}_i)\boldsymbol{\upsilon}_i. \tag{4}$$

Expressions (2), (3) and (4) allows to transform (1) to its corresponding operational space model, given by

$$\mathbf{M}_i(\mathbf{q}_i)\dot{\boldsymbol{\upsilon}}_i + \mathbf{C}_i(\mathbf{q}_i, \dot{\mathbf{q}}_i)\boldsymbol{\upsilon}_i + \mathbf{g}_i(\mathbf{q}_i) = \mathbf{f}_i \tag{5}$$

where $\mathbf{M}_i(\mathbf{q}_i) := \left(\mathbf{J}_i^\dagger\right)^\top \bar{\mathbf{M}}_i(\mathbf{q}_i)\mathbf{J}_i^\dagger$, $\mathbf{g}_i(\mathbf{q}_i) := \left(\mathbf{J}_i^\dagger\right)^\top \bar{\mathbf{g}}_i(\mathbf{q}_i)$, $\mathbf{C}_i(\mathbf{q}_i, \dot{\mathbf{q}}_i) := \left(\mathbf{J}_i^\dagger\right)^\top \left(\bar{\mathbf{M}}_i(\mathbf{q}_i)\dot{\mathbf{J}}_i^\dagger + \bar{\mathbf{C}}_i(\mathbf{q}_i, \dot{\mathbf{q}}_i)\mathbf{J}_i^\dagger\right)$.

The operational space model (5) has the following well-known properties (Spong et al., 2005):

P1. $\mathbf{M}_i(\mathbf{q}_i)$ is symmetric and there exist $\lambda_{m_i}, \lambda_{M_i} > 0$ such that $0 < \lambda_{m_i}\mathbf{I}_6 \leq \mathbf{M}_i(\mathbf{q}_i) \leq \lambda_{M_i}\mathbf{I}_6$.
P2. The matrix $\dot{\mathbf{M}}_i(\mathbf{q}_i) - 2\mathbf{C}_i(\mathbf{q}_i, \dot{\mathbf{q}}_i)$ is skew-symmetric.
P3. For all $\mathbf{q}_i, \dot{\mathbf{q}}_i, \boldsymbol{\upsilon}_i$, there exists $\eta_i \in \mathbb{R}_{>0}$ such that $|\mathbf{C}_i(\mathbf{q}_i, \dot{\mathbf{q}}_i)\boldsymbol{\upsilon}_i| \leq \eta_i|\boldsymbol{\upsilon}_i|^2$.
P4. If $\boldsymbol{\upsilon}_i, \dot{\boldsymbol{\upsilon}}_i \in \mathcal{L}_\infty$ then $\frac{d}{dt}\mathbf{C}_i(\mathbf{q}_i, \dot{\mathbf{q}}_i)$ is a bounded operator.

Using the total energy function $\mathcal{E}_i(\boldsymbol{\upsilon}_i, \mathbf{q}_i) = \mathcal{K}_i(\boldsymbol{\upsilon}_i) + \mathcal{U}_i(\mathbf{q}_i)$, where $\mathcal{K}_i$ is the kinetic energy given by

$$\mathcal{K}_i(\boldsymbol{\upsilon}_i) = \frac{1}{2}\boldsymbol{\upsilon}_i^\top \mathbf{M}_i(\mathbf{q}_i)\boldsymbol{\upsilon}_i, \tag{6}$$

and $\mathcal{U}_i$ is the gravity potential energy such that $\mathbf{g}_i(\mathbf{q}_i) := \frac{\partial \mathcal{U}_i}{\partial \mathbf{q}_i}$, it can be shown that (5) represents a passive map from force $\mathbf{f}_i$ to velocity $\boldsymbol{\upsilon}_i$.

2.2 Orientation in the SE(3)

A unit-quaternion $\boldsymbol{\xi}_i \in S^3$ can be split in two elements: one scalar term $\eta_i \in \mathbb{R}$ and one vectorial term $\boldsymbol{\beta}_i \in \mathbb{R}^3$. Thus $\boldsymbol{\xi}_i := [\eta_i, \boldsymbol{\beta}_i^\top]^\top$ and, from the unit norm constraint, $\eta_i^2 + \boldsymbol{\beta}_i^\top\boldsymbol{\beta}_i = 1$ (refer to (Chou, 1992) for a detailed list of properties and operations involving unit-quaternions).

[1] The set $S^3 \subset \mathbb{R}^4$ represents an unitary sphere of dimension three and it is defined as $S^3 := \{\boldsymbol{\xi} \in \mathbb{R}^4 : |\boldsymbol{\xi}|^2 = 1\}$.

The unit-quaternion $\boldsymbol{\xi}_i$ can be easily obtained from the direct kinematics function of each robot manipulator, via the rotation matrix $\mathbf{R}_i \in SO(3) := \{\mathbf{R}_i \in \mathbb{R}^{3\times 3} : \mathbf{R}_i^\top \mathbf{R}_i = \mathbf{I}_3, \det(\mathbf{R}_i) = 1\}$ (Spurrier, 1978; Spong et al., 2005).

The orientation error, relative to the world frame, between two different frames, $\boldsymbol{\Sigma}_i$ and $\boldsymbol{\Sigma}_j$, can be described by the rotation matrix $\tilde{\mathbf{R}}_{ij} := \mathbf{R}_i\mathbf{R}_j^\top \in SO(3)$. The unit-quaternion describing such orientation error is given by

$$\tilde{\boldsymbol{\xi}}_{ij} = \boldsymbol{\xi}_i \odot \boldsymbol{\xi}_j^* = \begin{bmatrix} \tilde{\eta}_{ij} \\ \tilde{\boldsymbol{\beta}}_{ij} \end{bmatrix} = \begin{bmatrix} \boldsymbol{\xi}_i^\top \boldsymbol{\xi}_j \\ \eta_j\boldsymbol{\beta}_i - \eta_i\boldsymbol{\beta}_j - \mathbf{S}(\boldsymbol{\beta}_i)\boldsymbol{\beta}_j \end{bmatrix} = \begin{bmatrix} \eta_i\eta_j + \boldsymbol{\beta}_i^\top\boldsymbol{\beta}_j \\ -\mathbf{U}^\top(\boldsymbol{\xi}_i)\boldsymbol{\xi}_j \end{bmatrix} \tag{7}$$

where $\odot$ denotes the quaternion product, $\boldsymbol{\xi}_{(\cdot)}^* = [\eta_{(\cdot)}, -\boldsymbol{\beta}_{(\cdot)}^\top]^\top$ is the quaternion conjugate, $\mathbf{S}(\cdot)$ is the skew-symmetric matrix operator [2] and $\mathbf{U}(\boldsymbol{\xi}_i)$ is defined as

$$\mathbf{U}(\boldsymbol{\xi}_i) := \begin{bmatrix} -\boldsymbol{\beta}_i^\top \\ \eta_i\mathbf{I}_3 - \mathbf{S}(\boldsymbol{\beta}_i) \end{bmatrix}. \tag{8}$$

The relation between the time-derivative of the unit-quaternion and the angular velocity, relative to the world reference frame, is given by

$$\dot{\boldsymbol{\xi}}_i = \frac{1}{2}\mathbf{U}(\boldsymbol{\xi}_i)\boldsymbol{\omega}_i. \tag{9}$$

Hence, defining $\boldsymbol{\Phi}(\boldsymbol{\xi}_i) := \mathrm{diag}(\mathbf{I}_3, \frac{1}{2}\mathbf{U}^\top(\boldsymbol{\xi}_i))$, it holds that

$$\dot{\mathbf{x}}_i = \boldsymbol{\Phi}^\top(\boldsymbol{\xi}_i)\boldsymbol{\upsilon}_i. \tag{10}$$

Using the normality condition, some straightforward calculations show that $\tilde{\boldsymbol{\beta}}_{ij} = \mathbf{0}$ if and only if $\boldsymbol{\xi}_i = \pm\boldsymbol{\xi}_j$. This, in turn, implies that $\mathbf{U}^\top(\boldsymbol{\xi}_i)\boldsymbol{\xi}_j = \mathbf{0}_3$. A key observation is that $\boldsymbol{\xi}_i = \boldsymbol{\xi}_j$ and $\boldsymbol{\xi}_i = -\boldsymbol{\xi}_j$ represent the same physical orientation. The following properties have been borrowed from (Fjellstad, 1994) and are used throughout the rest of the paper.

P5. For all $\boldsymbol{\xi}_i \in S^3$, $\mathbf{U}^\top(\boldsymbol{\xi}_i)\mathbf{U}(\boldsymbol{\xi}_i) = \mathbf{I}_3$. Hence, $\mathrm{rank}(\mathbf{U}(\boldsymbol{\xi}_i)) = 3$ and $\ker(\mathbf{U}^\top(\boldsymbol{\xi}_i)) = \mathrm{span}(\boldsymbol{\xi}_i)$.
P6. For all $\boldsymbol{\xi}_i \in S^3$ and $\dot{\boldsymbol{\xi}}_i \in \mathbb{R}^4$, $\dot{\mathbf{U}}(\boldsymbol{\xi}_i) = \mathbf{U}(\dot{\boldsymbol{\xi}}_i)$.
P7. Since, for all $\boldsymbol{\xi}_i \in S^3$, $|\boldsymbol{\xi}_i| = 1$ then $\mathbf{U}(\boldsymbol{\xi}_i)$ is a bounded operator.

2.3 Modeling the Interconnection

The interconnection of the N agents is modeled using the Laplacian matrix $\mathbf{L} := [\ell_{ij}] \in \mathbb{R}^{N\times N}$, whose elements are defined as

$$\ell_{ij} = \begin{cases} \sum\limits_{j\in\mathcal{N}_i} a_{ij} & i = j \\ -a_{ij} & i \neq j \end{cases} \tag{11}$$

where $\mathcal{N}_i$ is the set of agents transmitting information to the ith robot, $a_{ij} > 0$ if $j \in \mathcal{N}_i$ and $a_{ij} = 0$ otherwise.

Similar to passivity-based (energy-shaping) synchronization (Sarlette et al., 2009) and in order to ensure that the interconnection forces are generated by the gradient of a potential function, the following assumption is used in this paper:

A1. The interconnection graph is *undirected and connected*.

With regards to the interconnection time-delays it is assumed that

A2. The information exchange, from the j-th robot to the i-th robot, is subject to a variable time-delay $T_{ji}(t)$ with a known upper-bound ${}^*T_{ji}$. Hence, it holds that $0 \leq T_{ji}(t) \leq {}^*T_{ji} < \infty$. Additionally, the time–derivatives $\dot{T}_{ji}(t)$ are bounded.

If Assumptions **A1** and **A2** hold, then the interconnection graph exhibits the following properties (Olfati-Saber and Murray, 2004): **a)** $\mathbf{L}$ is symmetric and hence $\mathbf{L}^\top\mathbf{1}_N = \mathbf{0}_N$, **b)** The spectrum of $\mathbf{L}$ satisfies $\sigma(\mathbf{L}) \geq 0$, and $\sigma_m(\mathbf{L}) = 0$ has multiplicity one. Further, $\mathrm{rank}(\mathbf{L}) = N-1$, and **c)** For any $\mathbf{z} \in \mathbb{R}^N$, $\mathbf{z}^\top\mathbf{L}\mathbf{z} = \frac{1}{2}\sum\limits_{i\in\bar{N}}\sum\limits_{j\in\mathcal{N}_i} a_{ij}(z_i - z_j)^2 \geq 0$.

The Laplacian matrix models the followers interconnection and, in this work, a diagonal matrix $\mathbf{B} \in \mathbb{R}^{N\times N}$ is used to model the leader-follower interconnections. This paper has the following assumption for these interconnections:

A3. At least one of the N follower robots has direct access to the leader's constant pose $\mathbf{x}_\ell$, i.e., there exists at least one directed edge from the leader to any of the N followers.

Assumptions **A1** and **A3** ensure that the leader pose is *globally reachable* from any of the N follower nodes, *i.e.*, there exists a path from the leader to any ith follower robot. The following lemma provides an interesting property of the composed Laplacian matrix $\mathbf{L}_\ell := \mathbf{L} + \mathbf{B}$ that will be used in the proof of the main result and has been borrowed from Chapter 1, Lemma 1.6 of (Cao and Ren, 2011).

Lemma 1. (Cao and Ren, 2011) Consider a non-negative diagonal matrix $\mathbf{B} := \mathrm{diag}(b_{1\ell}, \ldots, b_{N\ell}) \in \mathbb{R}^{N\times N}$ and suppose that, at least, one $b_{i\ell}$ is strictly positive, i.e., there exists some $b_{i\ell} > 0$. Assume that **A1** holds, then the matrix $\mathbf{L}_\ell = \mathbf{L} + \mathbf{B}$ is symmetric, positive definite and of full rank. ◇

3. LEADER-FOLLOWER CONSENSUS

3.1 Problem Statement

In this paper is considered a network of N kinematically different EL-systems in the operational space of the form (5). It is assumed that the interconnection graph fulfills Assumptions **A1** and **A2**. The control objective is to design distributed control laws $\mathbf{f}_i$, such that the network of N followers has to be regulated at a given constant leader pose $\mathbf{x}_\ell := [\mathbf{p}_\ell^\top, \boldsymbol{\xi}_\ell^\top]^\top \subset \mathbb{R}^7$, provided that the leader pose is only available to a certain set of followers (**A3**). Hence, for all $i \in \bar{N}$,

$$\lim_{t\to\infty} |\boldsymbol{\upsilon}_i(t)| = 0, \quad \lim_{t\to\infty} \mathbf{x}_i(t) = \mathbf{x}_\ell. \tag{12}$$

3.2 Proposed Solution

The solution to the leader-follower consensus problem is established with the following operational space propor-

[2] For any $\mathbf{a}, \mathbf{b} \in \mathbb{R}^3$, $\mathbf{S}(\mathbf{a})\mathbf{b} = \mathbf{a} \times \mathbf{b}$. Some well known properties of the skew-symmetric matrix operator, $\mathbf{S}(\cdot)$, used throughout the paper are: $\mathbf{S}(\mathbf{a})^\top = \mathbf{S}(-\mathbf{a}) = -\mathbf{S}(\mathbf{a})$ and $\mathbf{S}(\mathbf{a})\mathbf{a} = \mathbf{0}_3$.

tional plus damping injection controller

$$\mathbf{f}_i = -k_i b_{i\ell}\mathbf{\Phi}(\boldsymbol{\xi}_i)(\mathbf{x}_i-\mathbf{x}_\ell)-k_i \sum_{j\in\mathcal{N}_i} a_{ij}\mathbf{\Phi}(\boldsymbol{\xi}_i)\mathbf{e}_{ij}-d_i\boldsymbol{\upsilon}_i+\mathbf{g}_i(\mathbf{q}_i) \quad (13)$$

where $k_i, d_i \in \mathbb{R}_{>0}$ are the controller gains, $b_{i\ell} > 0$ if the leader pose $\mathbf{x}_\ell$ is available to the ith robot manipulator and $b_{i\ell} = 0$, otherwise. The interconnection error $\mathbf{e}_{ij}$, for any pair of robots (i, j), is given by

$$\mathbf{e}_{ij} = \mathbf{x}_i - \mathbf{x}_j(t - T_{ji}(t)). \quad (14)$$

The closed-loop system (5) and (13) is

$$\dot{\boldsymbol{\upsilon}}_i = -\mathbf{M}_i^{-1}(\mathbf{q}_i)\Big[\mathbf{C}_i(\mathbf{q}_i,\dot{\mathbf{q}}_i)\boldsymbol{\upsilon}_i+d_i\boldsymbol{\upsilon}_i+k_i b_{i\ell}\mathbf{\Phi}(\boldsymbol{\xi}_i)(\mathbf{x}_i-\mathbf{x}_\ell) + k_i\sum_{j\in\mathcal{N}_i} a_{ij}\mathbf{\Phi}(\boldsymbol{\xi}_i)\mathbf{e}_{ij}\Big]. \quad (15)$$

It should be mentioned that, although $\boldsymbol{\xi}_i = \boldsymbol{\xi}_\ell$ and $\boldsymbol{\xi}_i = -\boldsymbol{\xi}_\ell$ represent the same physical orientation, the closed-loop system (15) has two possible equilibria. Proposition 2 formally states this fact and Proposition 3 shows that $\boldsymbol{\xi}_i = -\boldsymbol{\xi}_\ell$ corresponds to an unstable equilibrium point.

Proposition 2. If Assumptions **A1** and **A3** hold, then the closed-loop system (15) has the following two different equilibrium points, for all $i \in \bar{N}$,

$$(\boldsymbol{\upsilon}_i, \mathbf{p}_i, \boldsymbol{\xi}_i) = (\mathbf{0}_6, \mathbf{p}_\ell, \boldsymbol{\xi}_\ell) \quad (16)$$

and

$$(\boldsymbol{\upsilon}_i, \mathbf{p}_i, \boldsymbol{\xi}_i) = (\mathbf{0}_6, \mathbf{p}_\ell, -\boldsymbol{\xi}_\ell). \quad (17)$$

◇

Proof. The possible equilibria of (15), clearly satisfy $\boldsymbol{\upsilon}_i = \mathbf{0}_6$ and $b_{i\ell}\mathbf{e}_{i\ell} + \sum_{j\in\mathcal{N}_i} a_{ij}\mathbf{e}_{ij} = \mathbf{0}_6$, which in turn implies that

$$b_{i\ell}(\mathbf{p}_i - \mathbf{p}_\ell) + \sum_{j\in\mathcal{N}_i} a_{ij}(\mathbf{p}_i - \mathbf{p}_j(t - T_{ji}(t))) = \mathbf{0}_3, \quad (18)$$

$$-b_{i\ell}\mathbf{U}^\top(\boldsymbol{\xi}_i)\boldsymbol{\xi}_\ell - \sum_{j\in\mathcal{N}_i} a_{ij}\mathbf{U}^\top(\boldsymbol{\xi}_i)\boldsymbol{\xi}_j(t - T_{ji}(t)) = \mathbf{0}_3. \quad (19)$$

Now, $\mathbf{p}_j(t - T_{ji}(t)) = \mathbf{p}_j - \int_{t-T_{ji}(t)}^t \dot{\mathbf{p}}_j(\sigma)d\sigma$ and, at the equilibrium, $\int_{t-T_{ji}(t)}^t \dot{\mathbf{p}}_j(\sigma)d\sigma = \mathbf{0}_3$. This last, together with $\mathbf{p} := [\mathbf{p}_1^\top, \ldots, \mathbf{p}_N^\top]^\top$, allows to write (18) as

$$(\mathbf{B}_\ell \otimes \mathbf{I}_3)(\mathbf{p} - (\mathbf{1}_N \otimes \mathbf{p}_\ell)) + (\mathbf{L} \otimes \mathbf{I}_3)\mathbf{p} = \mathbf{0}_{3N}$$

and thus, since $\mathbf{L}\mathbf{1}_N = \mathbf{0}_N$, $(\mathbf{L}_\ell\otimes\mathbf{I}_3)(\mathbf{p}-(\mathbf{1}_N\otimes\mathbf{p}_\ell)) = \mathbf{0}_{3N}$, where $\mathbf{B}_\ell$ and $\mathbf{L}_\ell$ are defined in Lemma 1 and $\otimes$ is the standard Kronecker product. Further, Lemma 1 and the Kronecker product properties ensure that rank$(\mathbf{L}_\ell \otimes \mathbf{I}_3) = 3N$; thus, for all $i \in \bar{N}$, $\mathbf{p}_i = \mathbf{p}_\ell$ is the only solution to (18).

Similarly, $\boldsymbol{\xi}_j(t - T_{ji}(t)) = \boldsymbol{\xi}_j - \int_{t-T_{ji}(t)}^t \dot{\boldsymbol{\xi}}_j(\sigma)d\sigma$ and, at the equilibrium, $\int_{t-T_{ji}(t)}^t \dot{\boldsymbol{\xi}}_j(\sigma)d\sigma = \mathbf{0}_4$. Thus, (19) can be written as

$$-b_{i\ell}\mathbf{U}^\top(\boldsymbol{\xi}_i)\boldsymbol{\xi}_\ell - \sum_{j\in\mathcal{N}_i} a_{ij}\mathbf{U}^\top(\boldsymbol{\xi}_i)\boldsymbol{\xi}_j = \mathbf{0}_3.$$

Adding the term $b_{i\ell}\mathbf{U}^\top(\boldsymbol{\xi}_i)\boldsymbol{\xi}_i + \sum_{j\in\mathcal{N}_i} a_{ij}\mathbf{U}^\top(\boldsymbol{\xi}_i)\boldsymbol{\xi}_i$ to the previous equation, with the fact that $\mathbf{U}^\top(\boldsymbol{\xi}_i)\boldsymbol{\xi}_i = \mathbf{0}_3$, yields

$$b_{i\ell}\mathbf{U}^\top(\boldsymbol{\xi}_i)(\boldsymbol{\xi}_i - \boldsymbol{\xi}_\ell) + \sum_{j\in\mathcal{N}_i} a_{ij}\mathbf{U}^\top(\boldsymbol{\xi}_i)(\boldsymbol{\xi}_i - \boldsymbol{\xi}_j) = \mathbf{0}_3. \quad (20)$$

Defining $\boldsymbol{\xi} := [\boldsymbol{\xi}_1^\top, \ldots, \boldsymbol{\xi}_N^\top]^\top$ and $\bar{\mathbf{U}} := \mathrm{diag}(\mathbf{U}(\boldsymbol{\xi}_1), \ldots, \mathbf{U}(\boldsymbol{\xi}_N)) \in \mathbb{R}^{4N\times 3N}$, (20) can be written as

$$\bar{\mathbf{U}}^\top [(\mathbf{B}_\ell \otimes \mathbf{I}_4)(\boldsymbol{\xi} - (\mathbf{1}_N \otimes \boldsymbol{\xi}_\ell)) + (\mathbf{L} \otimes \mathbf{I}_4)\boldsymbol{\xi}] = \mathbf{0}_{3N}$$

Using $\mathbf{L}\mathbf{1}_N = \mathbf{0}_N$, this last equations is equivalent to

$$\bar{\mathbf{U}}^\top(\mathbf{L}_\ell \otimes \mathbf{I}_4)(\boldsymbol{\xi} - (\mathbf{1}_N \otimes \boldsymbol{\xi}_\ell)) = \mathbf{0}_{3N}$$

Finally, since $(\mathbf{L}_\ell \otimes \mathbf{I}_4)$ is of full rank then the trivial solution $\boldsymbol{\xi} = \mathbf{1}_N \otimes \boldsymbol{\xi}_\ell$ satisfies this equation. However, the fact that rank$(\bar{\mathbf{U}}) = 3N$ and **P5** ensure that $\boldsymbol{\xi}_i = \pm\boldsymbol{\xi}_\ell$, for all $i \in \bar{N}$.

At this point the main result of this work can be stated.

Proposition 3. Under Assumptions **A1**, **A2** and **A3**, controller (13) solves the leader-follower consensus problem provided that, for any $\alpha_i, \alpha_j > 0$, damping d_i satisfies

$$2d_i > k_i\ell_{ii}\alpha_i + k_i \sum_{j\in\mathcal{N}_i} a_{ji}\frac{{}^*T_{ji}^2}{\alpha_j}, \quad \forall i \in \bar{N}. \quad (21)$$

Furthermore, the equilibrium (17) is unstable and the equilibrium (16) is asymptotically stable everywhere except at $(\mathbf{0}_6, \mathbf{p}_\ell, -\boldsymbol{\xi}_\ell)$. ◇

Proof. The closed-loop system (15) exhibits the following (scaled) energy

$$\mathcal{V}_i := \frac{1}{k_i}\mathcal{K}_i(\boldsymbol{\upsilon}_i) + \frac{b_{i\ell}}{2}|\mathbf{x}_i - \mathbf{x}_\ell|^2 + \frac{1}{4}\sum_{j\in\mathcal{N}_i} a_{ij}|\mathbf{x}_i - \mathbf{x}_j|^2 \quad (22)$$

where $\mathcal{K}_i$ has been defined in (6). Note that $\mathcal{V}_i$ is positive definite and radially unbounded with regards to $\boldsymbol{\upsilon}_i, |\mathbf{x}_i - \mathbf{x}_\ell|$ and $|\mathbf{x}_i - \mathbf{x}_j|$, for all $i \in \bar{N}$ and $j \in \mathcal{N}_i$.

Using (10), Property (**P2**) and the fact that $\dot{\mathbf{x}}_\ell = \mathbf{0}_7$ ensure that $\dot{\mathcal{V}}_i$, evaluated along (15), is given by

$$\begin{aligned}\dot{\mathcal{V}}_i =& -\frac{d_i}{k_i}|\boldsymbol{\upsilon}_i|^2 - \sum_{j\in\mathcal{N}_i} a_{ij}\left[\dot{\mathbf{x}}_i^\top\mathbf{e}_{ij} - \frac{1}{2}(\dot{\mathbf{x}}_i - \dot{\mathbf{x}}_j)^\top(\mathbf{x}_i - \mathbf{x}_j)\right]\\ =& -\frac{d_i}{k_i}|\boldsymbol{\upsilon}_i|^2 - \sum_{j\in\mathcal{N}_i} a_{ij}\dot{\mathbf{x}}_i^\top\int_{t-T_{ji}(t)}^t \dot{\mathbf{x}}_j(\sigma)d\sigma -\\ & -\frac{1}{2}\sum_{j\in\mathcal{N}_i} a_{ij}(\dot{\mathbf{x}}_i + \dot{\mathbf{x}}_j)^\top(\mathbf{x}_i - \mathbf{x}_j)\end{aligned}$$

Adding and subtracting the term $\mathbf{x}_i^\top\dot{\mathbf{x}}_i$ and doing some algebra, yields

$$\begin{aligned}(\dot{\mathbf{x}}_i + \dot{\mathbf{x}}_j)^\top(\mathbf{x}_i - \mathbf{x}_j) =& \dot{\mathbf{x}}_i^\top(\mathbf{x}_i - \mathbf{x}_j) - \mathbf{x}_i^\top(\dot{\mathbf{x}}_i - \dot{\mathbf{x}}_j) + \mathbf{x}_i^\top\dot{\mathbf{x}}_i\\ & - \mathbf{x}_j^\top\dot{\mathbf{x}}_j\\ =& \dot{\mathbf{x}}_i^\top(\mathbf{x}_i - \mathbf{x}_j) - \mathbf{x}_i^\top(\dot{\mathbf{x}}_i - \dot{\mathbf{x}}_j) + \rho_i - \rho_j\end{aligned}$$

where the scalar $\rho_{(\cdot)}$ is defined as $\rho_{(\cdot)} := \mathbf{x}_{(\cdot)}^\top\dot{\mathbf{x}}_{(\cdot)}$. Now, using (11) and since $\sum_{i\in\bar{N}}\sum_{j\in\mathcal{N}_i} a_{ij}(\rho_i - \rho_j) = \mathbf{1}_N^\top\mathbf{L}\boldsymbol{\rho} = 0$, it is straightforward to show that

$$\sum_{i\in\bar{N}}\sum_{j\in\mathcal{N}_i} a_{ij}(\dot{\mathbf{x}}_i+\dot{\mathbf{x}}_j)^\top(\mathbf{x}_i-\mathbf{x}_j) = \mathbf{x}^\top\left((\mathbf{L}^\top - \mathbf{L})\otimes\mathbf{I}_7\right)\dot{\mathbf{x}} = 0$$

where $\boldsymbol{\rho} := [\rho_1, \ldots, \rho_N]^\top \in \mathbb{R}^N$ and $\mathbf{x} := [\mathbf{x}_1^\top, \ldots, \mathbf{x}_N^\top]^\top$, $\dot{\mathbf{x}} := [\dot{\mathbf{x}}_1^\top, \ldots, \dot{\mathbf{x}}_1^\top]^\top \in \mathbb{R}^{7N}$. Hence, taking $\mathcal{V} = \sum_{i\in\bar{N}}\mathcal{V}_i$ it holds that

$$\dot{\mathcal{V}} = -\sum_{i\in\bar{N}}\left[\frac{d_i}{k_i}|\boldsymbol{\upsilon}_i|^2 + \sum_{j\in\mathcal{N}_i} a_{ij}\dot{\mathbf{x}}_i^\top\int_{t-T_{ji}(t)}^t \dot{\mathbf{x}}_j(\sigma)d\sigma\right]$$

Since $\mathcal{V}$ does not qualify as a Lyapunov Function, i.e., $\dot{\mathcal{V}} < 0$, in the same spirit as in (Nuño et al., 2013), it is possible to integrate $\dot{\mathcal{V}}$ from 0 to t and then apply Lemma 1 in (Nuño et al., 2009) to the double integral terms. Furthermore, from (9), it can be inferred that $4|\dot{\boldsymbol{\xi}}_i|^2 = |\boldsymbol{\omega}_i|^2$ thus, using $|\boldsymbol{\upsilon}_i|^2 = |\dot{\mathbf{x}}_i|^2 + 3|\dot{\boldsymbol{\xi}}_i|^2$, yields

$$\mathcal{V}(t) - \mathcal{V}(0) = -\sum_{i\in\bar{N}} \frac{d_i}{k_i}\left[\int_0^t |\dot{\mathbf{x}}_i(\theta)|^2 d\theta + 3\int_0^t |\dot{\boldsymbol{\xi}}_i(\theta)|^2 d\theta\right] - \sum_{i\in\bar{N}}\sum_{j\in\mathcal{N}_i} a_{ij}\int_0^t \dot{\mathbf{x}}_i^\top(\theta)\int_{\theta-T_{ji}(\theta)}^{\theta} \dot{\mathbf{x}}_j(\sigma)d\sigma d\theta,$$

and, for any $\alpha_i > 0$ and $i \in \bar{N}$,

$$\mathcal{V}(t) - \mathcal{V}(0) \le -\sum_{i\in\bar{N}} \frac{d_i}{k_i}\left(\|\dot{\mathbf{x}}_i\|_2^2 + 3\|\dot{\boldsymbol{\xi}}_i\|_2^2\right) + \sum_{i\in\bar{N}}\sum_{j\in\mathcal{N}_i} a_{ij}\left(\frac{\alpha_i}{2}\|\dot{\mathbf{x}}_i\|_2^2 + \frac{{}^*T_{ji}^2}{2\alpha_j}\|\dot{\mathbf{x}}_j\|_2^2\right).$$

Moreover, recalling that $\ell_{ii} = \sum_{j\in\mathcal{N}_i} a_{ij}$ then it holds that

$$\mathcal{V}(t) - \mathcal{V}(0) \le -\sum_{i\in\bar{N}} \frac{3d_i}{k_i}\|\dot{\boldsymbol{\xi}}_i\|_2^2 + \sum_{i\in\bar{N}}\sum_{j\in\mathcal{N}_i} a_{ij}\frac{{}^*T_{ji}^2}{2\alpha_j}\|\dot{\mathbf{x}}_j\|_2^2 - \sum_{i\in\bar{N}}\sum_{j\in\mathcal{N}_i} a_{ij}\left(\frac{d_i}{k_i\ell_{ii}} - \frac{\alpha_i}{2}\right)\|\dot{\mathbf{x}}_i\|_2^2,$$

which can be further written as

$$\mathcal{V}(t) + \sum_{i\in\bar{N}} \frac{3d_i}{k_i}\|\dot{\boldsymbol{\xi}}_i\|_2^2 + \mathbf{1}_N^\top \boldsymbol{\Psi}\left[\|\dot{\mathbf{x}}_1\|_2^2, \ldots, \|\dot{\mathbf{x}}_N\|_2^2\right]^\top \le \mathcal{V}(0)$$

where

$$\boldsymbol{\Psi} = \begin{bmatrix} \frac{d_1}{k_1} - \frac{\ell_{11}\alpha_1}{2} & -\frac{a_{12}{}^*T_{21}^2}{2\alpha_1} & \cdots & -\frac{a_{1N}{}^*T_{N1}^2}{2\alpha_1} \\ -\frac{a_{21}{}^*T_{12}^2}{2\alpha_2} & \frac{d_2}{k_2} - \frac{\ell_{22}\alpha_2}{2} & \cdots & -\frac{a_{2N}{}^*T_{N2}^2}{2\alpha_2} \\ \vdots & \vdots & \ddots & \vdots \\ -\frac{a_{N1}{}^*T_{1N}^2}{2\alpha_N} & -\frac{a_{N2}{}^*T_{2N}^2}{2\alpha_N} & \cdots & \frac{d_N}{k_N} - \frac{\ell_{NN}\alpha_N}{2} \end{bmatrix}.$$

Clearly, if d_i is set according to (21) then there exists $\boldsymbol{\mu} \in \mathbb{R}^N$, defined as $\boldsymbol{\mu} := \boldsymbol{\Psi}^\top \mathbf{1}_N$, such that $\mu_i > 0$, for all $i \in \bar{N}$. Hence

$$\mathcal{V}(t) + \sum_{i\in\bar{N}}\left(\frac{3d_i}{k_i}\|\dot{\boldsymbol{\xi}}_i\|_2^2 + \mu_i\|\dot{\mathbf{x}}_i\|_2^2\right) \le \mathcal{V}(0).$$

Therefore, $\dot{\mathbf{x}}_i \in \mathcal{L}_2$ and $\mathcal{V} \in \mathcal{L}_\infty$. This last implies that $\boldsymbol{\upsilon}_i, |\mathbf{x}_i - \mathbf{x}_\ell|, |\mathbf{x}_i - \mathbf{x}_j| \in \mathcal{L}_\infty$, for all $i \in \bar{N}$ and $j \in \mathcal{N}_i$. All these bounded signals together with Property (**P3**) and the fact that $|\boldsymbol{\xi}_i| = 1$ ensure, from the closed-loop system (15), that $\dot{\boldsymbol{\upsilon}} \in \mathcal{L}_\infty$. Additionally, from (9), $\dot{\mathbf{x}}_i \in \mathcal{L}_2$ implies that $\boldsymbol{\upsilon}_i \in \mathcal{L}_2$. Barbălat's Lemma with $\boldsymbol{\upsilon}_i \in \mathcal{L}_\infty \cap \mathcal{L}_2$ and $\dot{\boldsymbol{\upsilon}}_i \in \mathcal{L}_\infty$ supports the fact that $\lim_{t\to\infty} \boldsymbol{\upsilon}_i(t) = \mathbf{0}_6$, which in turn implies from (9) that $\lim_{t\to\infty} \dot{\mathbf{x}}_i(t) = \mathbf{0}_7$.

Boundedness of $\dot{\boldsymbol{\upsilon}}_i$, $\boldsymbol{\upsilon}_i$, $|\mathbf{x}_i - \mathbf{x}_\ell|$ and $|\mathbf{x}_i - \mathbf{x}_j|$, together with Property (**P4**), imply that $\dot{\boldsymbol{\upsilon}}_i$ is uniformly continuous. Moreover, since

$$\lim_{t\to\infty}\int_0^t \dot{\boldsymbol{\upsilon}}_i(\sigma)d\sigma = \lim_{t\to\infty} \boldsymbol{\upsilon}_i(t) - \boldsymbol{\upsilon}_i(0) = -\boldsymbol{\upsilon}_i(0),$$

then $\lim_{t\to\infty} \dot{\boldsymbol{\upsilon}}_i(t) = \mathbf{0}_6$.

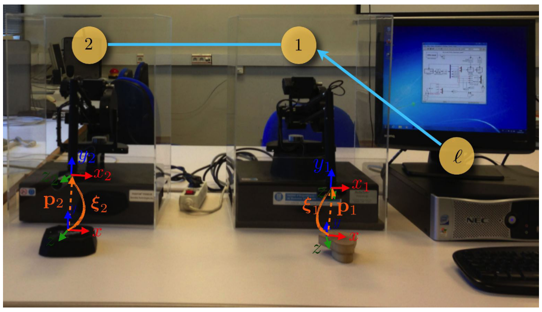

Fig. 2. Experimental validation setup.

Invoking Proposition 2 it holds that, when $\lim_{t\to\infty} \boldsymbol{\upsilon}_i(t) = \lim_{t\to\infty} \dot{\boldsymbol{\upsilon}}_i(t) = \mathbf{0}_6$, the closed-loop system (15) has only two possible equilibrium points, namely (16) and (17). Using (22) it is shown that (16) corresponds to a minimum energy point and since $\mathcal{V}(t)$ is a decreasing function, *i.e.*, $\mathcal{V}(t) \le \mathcal{V}(0)$, any perturbation from (17) will drive the system to (16). Hence, $(\boldsymbol{\upsilon}_i, \mathbf{p}_i, \boldsymbol{\xi}_i) = (\mathbf{0}_6, \mathbf{p}_\ell, \boldsymbol{\xi}_\ell)$ is asymptotically stable everywhere except at the unstable equilibrium point (17). This concludes the proof.

4. EXPERIMENTAL VALIDATION

The experimental setup is shown in the Fig. 2, and it is composed of two robots with 6-DoF, one PHANTOM Premium 1.5 High Force® and one PHANTOM Premium 1.5® with their control computers interconnected through a local area network. These robots are commercially available from Geomagic®. The controllers have been programmed using Matlab version 7.11 and Simulink version 7.6. The communications between Simulink and the robots make use of a custom library, called *PhanTorque 6Dof* [3]. This library allows to directly set the torques of the 6-DoF in the PHANTOM Premium models, and it also returns the transformation matrix of the robots end-effector. The data transmission of the robots' pose is done through UDP ports and, to emulate a transcontinental communication, a couple of artificially induced delays have been added (Salvo Rossi et al., 2006). The gravitational torque vectors and the estimated values of the two Premium devices, can be found in (Aldana et al., 2013). The Jacobian matrix is detailed in (Rodriguez and Basañez, 2005).

The two PHANTOM robots define the followers network and the leader constant pose is sent only to Node 1, thus $\bar{N} := \{1, 2\}$, $b_{1\ell} = 1$ and $b_{2\ell} = 0$. The resulting leader-follower interconnection can be seen in the Fig. 2. The interconnection weights are set to: $a_{12} = a_{21} = 0.6$, the proportional and damping injection gains are fixed to: k_1=10, d_1=1.4, k_2=7, d_2=1.25, and the upper bounds of the induced variable time delays are: ${}^*T_{21}$=0.19s and ${}^*T_{12}$=0.25s. Setting α_1=0.3, α_2=0.35 ensures that (21) holds. Despite the initial poses differences and the variable time-delays in the interconnection, both robot poses ($\mathbf{x}_1$ and $\mathbf{x}_2$) asymptotically reach the leader pose ($\mathbf{x}_\ell$) as can be seen In the Fig. 3 and the Fig. 4. Furthermore, from Fig. 5, it can be observed that pose errors asymptotically converge to zero. These experimental results verify the theoretical results of Proposition 3.

[3] The libraries are publicly available at http://sir.upc.edu/wikis/roblab/index.php/Projects/PhanTorqueLibraries

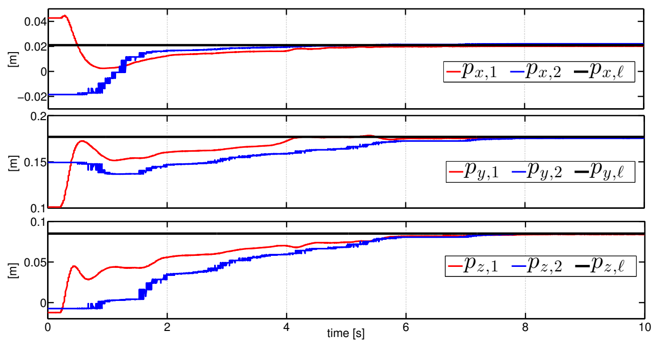

Fig. 3. Robots' position.

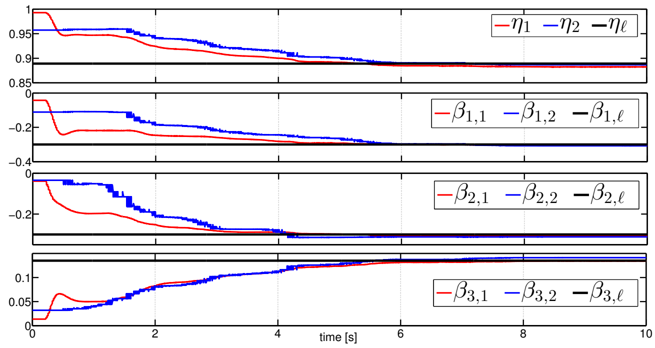

Fig. 4. Robots' orientation (Unit-quaternions).

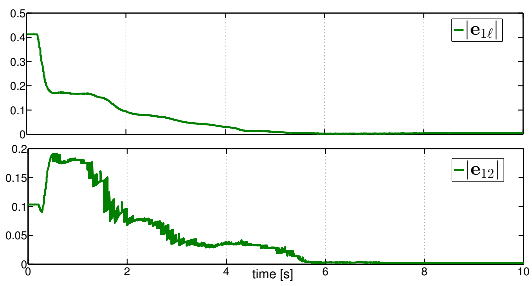

Fig. 5. Pose errors.

5. CONCLUSION

This paper presents a controller that solves the leader-follower operational space consensus problem in networks composed of multiple robot manipulators. It is proved that, with a simple decentralized proportional plus damping controller and sufficiently large damping the network asymptotically reach a consensus pose at the given leader pose. Both, the dynamics and the controller are defined in the operational space using unit quaternions to represent the orientation. Furthermore, it is shown that the controller is robust to interconnection variable time-delays. Experiments, with a network of two 6-DoF robot manipulators, are shown to support the theoretical results of this paper. Future research avenues span the development of adaptive controllers for the estimation of the gravity terms.

REFERENCES

A. Abdessameud and A. Tayebi. On consensus algorithms design for double integrator dynamics. *Automatica*, 49 (1):253–260, 2013.

A. Abdessameud, A. Tayebi, and I.-G. Polushin. Attitude synchronization of multiple rigid bodies with communication delays. *IEEE Trans. Autom. Control*, 57(9): 2405–2411, 2012.

C. Aldana, E. Nuño, and L. Basañez. Bilateral teleoperation of cooperative manipulators. In *IEEE Int. Conf. Robot. Autom.*, pages 4274 –4279, may 2012.

C. I. Aldana, E. Nuño, and L. Basañez. Control of bilateral teleoperators in the operational space without velocity measurements. In *IEEE/RSJ Int. Conf. on Intell. Robots and Syst.*, 2013.

Y. Cao and W. Ren. *Distributed Coordination of Multi-agent Networks: Emergent Problems, Models, and Issues*. Springer-Verlag, 2011.

J. C. K. Chou. Quaternion kinematic and dynamic differential equations. *IEEE Trans. Robot. Autom.*, 8 (1):53–64, 1992.

O. E. Fjellstad. *Control of unmanned underwater vehicles in six degrees of freedom: a quaternion feedback approach*. PhD thesis, Norwegian Institute of Technology, University of Trondheim, 1994.

H.-X. Hu, L. Yu, W.-A. Zhang, and H. Song. Group consensus in multi-agent systems with hybrid protocol. *J. Franklin Inst.*, 350(3):575–597, 2013.

Y.C. Liu and N. Chopra. Controlled synchronization of heterogeneous robotic manipulators in the task space. *IEEE Trans. Robot.*, 28(1):268–275, feb. 2012.

E. Nuño, L. Basañez, R. Ortega, and M. W. Spong. Position tracking for nonlinear teleoperators with variable time-delay. *Int. J. Robot. Res.*, 28(7):895–910, July 2009.

E. Nuño, I. Sarras, and L. Basañez. Consensus in networks of nonidentical Euler-Lagrange systems using P+d controllers. *IEEE Transactions on Robotics*, 26(6):1503–1508, 2013.

R. Olfati-Saber and R.M. Murray. Consensus problems in networks of agents with switching topology and time-delays. *IEEE Trans. Autom. Control*, 49(9):1520–1533, Sept. 2004.

W. Ren. Distributed attitude alignment in spacecraft formation flying. *Int. J. Adapt. Contr. Signal Process.*, 21(2-3):95–113, 2007.

A. Rodriguez and L. Basañez. Modelo cinemático de la interfase háptica PHANToM 1.5/6DOF (http://upcommons.upc.edu/pfc/handle/2099.1/14587). Technical report, Institute of Industrial and Control Engineering, Technical University of Catalonia, 2005.

P. Salvo Rossi, G. Romano, F. Palmieri, and G. Iannello. Joint end-to-end loss-delay hidden markov model for periodic udp traffic over the internet. *IEEE Trans. Sign. Proc.*, 54(2):530–541, 2006.

A. Sarlette, R. Sepulchre, and N. E. Leonard. Autonomous rigid body attitude synchronization. *Automatica*, 45(2): 572–577, 2009.

M. W. Spong, S. Hutchinson, and M. Vidyasagar. *Robot Modeling and Control*. Wiley, 2005. ISBN 978-0-471-64990-8.

R. A. Spurrier. Comment on singularity-free extraction of a quaternion from a direction-cosine matrix. *J. Spacecraft and Rockets*, 15(4):255, 1978.

Y. Sun. Average consensus in networks of dynamic agents with uncertain topologies and time-varying delays. *J. Franklin Inst.*, 349(3):1061–1073, 2012.